

# Thallium Nuclear Magnetic Relaxation in Solid Thallium(I) Thiocyanate TlSCN: Phase Transition and Ionic Motion

Yoshihiro Furukawa and Daiyu Nakamura

Department of Chemistry, Faculty of Science, Nagoya University, Nagoya, Japan

Z. Naturforsch. **45a**, 1211–1216 (1990); received July 20, 1990

The NMR spin-lattice relaxation time ( $T_1$ ) and linewidth parameter ( $T_2^*$ ) of  $^{203}\text{Tl}$  and  $^{205}\text{Tl}$  in solid TlSCN were measured from 290 K up to the melting point ( $T_m = 507\text{ K}$ ). The nonexponential magnetization recovery of  $T_1$  could be characterized by a short ( $T_1^s$ ) and a long ( $T_1^l$ ) component.  $T_1^l$  showed a  $T^{-2}$  dependence below ca. 350 K in the orthorhombic phase ( $T < T_c = 371\text{ K}$ ) and a minimum in the tetragonal phase ( $T_c < T < T_m$ ), which were interpreted in terms of lattice vibrations and head-to-tail flips of the linear  $\text{SCN}^-$  ions, respectively. A broad minimum of  $T_1^s$  around 360 K was explained in terms of indirect nucleus-electron scalar coupling between  $^{203}\text{Tl}$  and  $^{205}\text{Tl}$ , modulated via the anionic flips occurring in the symmetric and asymmetric potential fields for the high- and low-temperature phase, respectively. The phase transition is closely related to dynamical disorder of the anionic orientations. At higher temperatures, translational self-diffusion of  $\text{Tl}^+$  was evidenced by the  $T_2^*$  and  $T_1^s$  results.

## Introduction

It is known that many thiocyanate compounds with monovalent cations undergo interesting phase transitions [1–12]. Among them, the phase transition from orthorhombic to tetragonal KSCN is related to head-to-tail ordering of the rod-like  $\text{SCN}^-$  ions [1–8]. In the high-temperature phase, the anions jump between two equivalent orientations while in the low-temperature phase they form an ordered antiparallel arrangement [3, 7].

Thallium thiocyanate TlSCN undergoes a phase transition at ca. 370 K [9, 10], where a mechanism similar to that of KSCN is assumed on the basis of the low- and high-temperature structures [10] and the entropy change of transition [9]. For solid  $\text{TlNO}_2$ , the nuclear magnetic relaxation of Tl gives information on the motion of not only  $\text{Tl}^+$  but also the anions through the strong scalar coupling between  $^{203}\text{Tl}$  and  $^{205}\text{Tl}$ , modulated by the anionic motions [13]. In order to get similar information on TlSCN, we measured its temperature dependences of the spin-lattice relaxation time ( $T_1$ ) and linewidth parameter ( $T_2^*$ ) of both  $^{203}\text{Tl}$  and  $^{205}\text{Tl}$ .

## Experimental

We used a pulse NMR spectrometer already reported [14].  $T_1$  was measured by the usual  $180^\circ - t - 90^\circ$  pulse sequence and  $T_2^*$  from the free induction decay signal. In order to identify the sample, DTA was carried out with a homemade apparatus [15] and X-ray powder analysis with a Shimadzu VD-1A diffractometer. Temperatures were determined within  $\pm 1\text{ K}$ .

TlSCN was prepared by mixing aqueous solutions of  $\text{NH}_4\text{SCN}$  and  $\text{TlOH}$ , subsequent heating to remove  $\text{NH}_3$  gas [16] and recrystallization. For the NMR experiments, two types of the samples were used: One was finely powdered and the other partially melted to improve the filling factor. Because both samples yielded experimentally the same relaxation times, the NMR experiments were mainly carried out on the latter sample.

## Experimental Results

From our DTA experiments we found the phase transition temperature  $T_c = 371\text{ K}$  and the melting point  $T_m = 507\text{ K}$ . These values are in better agreement with  $T_c = 372\text{ K}$  and  $T_m = 507\text{ K}$  in [9] than those in [10]. The heat anomaly showed a long tail on the low-temperature side characteristic of a second-order phase transition, but a small latent heat was clearly observed indicating that the transition is of first order.

Reprint requests to Dr. Yoshihiro Furukawa, Department of Chemistry, Faculty of Science, Nagoya University, Nagoya 464-01, Japan.

0932-0784 / 90 / 0900-1211 \$ 01.30/0. – Please order a reprint rather than making your own copy



Dieses Werk wurde im Jahr 2013 vom Verlag Zeitschrift für Naturforschung in Zusammenarbeit mit der Max-Planck-Gesellschaft zur Förderung der Wissenschaften e.V. digitalisiert und unter folgender Lizenz veröffentlicht: Creative Commons Namensnennung-Keine Bearbeitung 3.0 Deutschland Lizenz.

Zum 01.01.2015 ist eine Anpassung der Lizenzbedingungen (Entfall der Creative Commons Lizenzbedingung „Keine Bearbeitung“) beabsichtigt, um eine Nachnutzung auch im Rahmen zukünftiger wissenschaftlicher Nutzungsformen zu ermöglichen.

This work has been digitalized and published in 2013 by Verlag Zeitschrift für Naturforschung in cooperation with the Max Planck Society for the Advancement of Science under a Creative Commons Attribution-NoDerivs 3.0 Germany License.

On 01.01.2015 it is planned to change the License Conditions (the removal of the Creative Commons License condition “no derivative works”). This is to allow reuse in the area of future scientific usage.

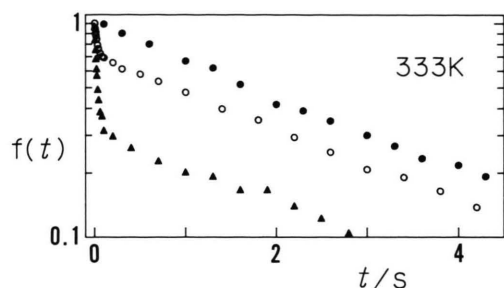


Fig. 1. Typical magnetization recovery curves  $f(t) = \{M_0 - M_z(t)\} / c M_0$  in the  $T_1$  measurements (16 MHz and 333 K). Here,  $M_0$  represents the equilibrium value of the nuclear magnetization.  $c$  equals 1 or 2 for the saturation pulse method or the  $180^\circ$ - $t$ - $90^\circ$  pulse method, respectively.  $\blacktriangle$  and  $\circ$ :  $^{203}\text{Tl}$  and  $^{205}\text{Tl}$  for the  $180^\circ$ - $t$ - $90^\circ$  pulse method, respectively.  $\bullet$ :  $^{205}\text{Tl}$  for the saturation pulse method. Since the saturation pulses for  $^{203}\text{Tl}$  or  $^{205}\text{Tl}$  decouple magnetically the two spin systems because of their very close resonance frequencies [19], the magnetization recovery after the pulses becomes exponential.

The room-temperature NMR frequency of  $^{205}\text{Tl}$  in solid TISCN was found to be low-field shifted by ca. 420 ppm as compared to that of an aqueous solution of  $\text{TlNO}_3$ . The temperature dependence of  $T_1$  of  $^{203}\text{Tl}$  and  $^{205}\text{Tl}$  was measured at the resonance frequencies 32 and 16 MHz. Except for above ca. 450 K and at 32 MHz, the magnetization recovery after the  $180^\circ$  pulse was very nonexponential. This may be due to the strong coupling of the spin systems of  $^{203}\text{Tl}$  and  $^{205}\text{Tl}$ , because of their resonance frequencies being very close [13, 17–20]. Typical magnetization recovery curves are shown in Figure 1. The nonexponential  $T_1$  decay was decomposed into a long ( $T_1^l$ ) and a short ( $T_1^s$ ) exponential relaxation time. The results are shown in Figure 2.

With increasing the temperature from room temperature,  $T_1^l$  gradually decreased up to ca. 400 K, a change of the temperature coefficient being recognized near 350 K. In this temperature range, no frequency dependence was observed. On further heating,  $T_1^l$  for  $^{205}\text{Tl}$  at 16 MHz yielded a shallow minimum around 430 K, at 32 MHz a minimum of ca. 0.4 s near 460 K. It is noted that the  $T_1^l$  minimum at the higher frequency is deeper than that at the lower frequency, in contrast to the expectation from the usual BPP theory of the magnetic dipolar relaxation [20]. When  $T_1^l$  was measured at 32 MHz and above ca. 450 K, the magnetization recovery became almost exponential and gave a single  $T_1^l$  value. In the whole temperature range studied,  $T_1^l$  is likely to have no isotope dependence.

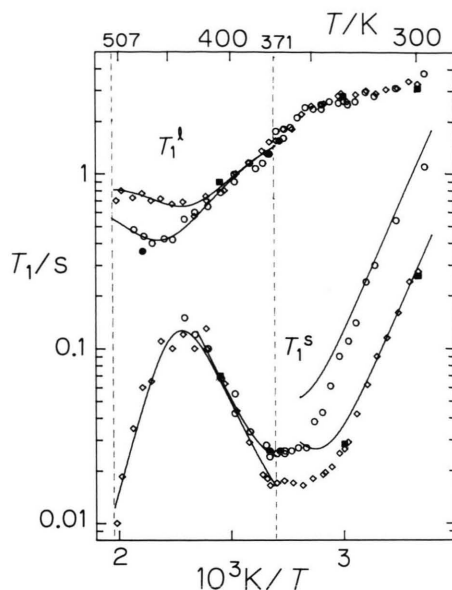


Fig. 2. Temperature dependence of the  $^{203}\text{Tl}$  and  $^{205}\text{Tl}$  spin-lattice relaxation times in solid TISCN. Solid lines: Calculated with the theoretical expressions given in the text.

| Symbols: | $^{203}\text{Tl}$ | $^{205}\text{Tl}$ |
|----------|-------------------|-------------------|
| 16 MHz   | $\blacksquare$    | $\diamond$        |
| 32 MHz   | $\bullet$         | $\circ$           |

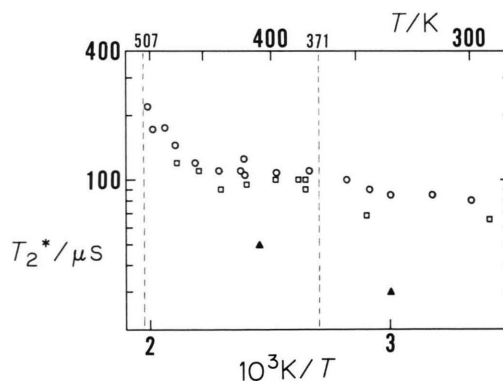


Fig. 3. Temperature variation of the linewidth parameter  $T_2^*$ .

| Symbols: | $^{203}\text{Tl}$ | $^{205}\text{Tl}$ |
|----------|-------------------|-------------------|
| 16 MHz   | $\blacktriangle$  | $\circ$           |
| 32 MHz   |                   | $\square$         |

On the other hand,  $T_1^s$  at 32 MHz sharply decreased with increasing temperature to ca. 350 K and became almost temperature independent from 350 K to  $T_c$ . A clear frequency dependence of  $T_1^s$  was observed in the room-temperature phase (phase II). For the high-tem-

perature phase (phase I),  $T_1^s$  at both 32 and 16 MHz increased with increasing temperature up to ca. 435 K. On further heating,  $T_1^s$  at 16 MHz sharply decreased while at 32 MHz it could not be determined, as mentioned above. In a narrow temperature range just above  $T_c$ , a small frequency dependence was recognized.  $T_1^s$  showed no isotope dependence in the whole temperature range studied as well.

Figure 3 shows the temperature variation of  $T_2^*$ .  $^{205}\text{Tl}$   $T_2^*$  at 16 MHz was almost constant at ca. 85  $\mu\text{s}$  below 350 K and at ca. 110  $\mu\text{s}$  between  $T_c$  and 450 K, and increased rather steeply above 450 K.  $T_2^*$  of  $^{205}\text{Tl}$  at 32 MHz was slightly smaller than that at 16 MHz. For  $^{203}\text{Tl}$ ,  $T_2^*$  was found to be shorter by a factor of 2–3 than that of  $^{205}\text{Tl}$  at a given frequency and temperature.

## Analysis of the Results and Discussion

We will consider electron-nuclear magnetic coupling which is known to play an important role in Tl ( $I=1/2$ ) NMR [13, 17–20]. Normal nuclear magnetic dipolar interaction can be neglected according to the usual BPP theory of  $T_1$  for a model of complete motional averaging of the dipolar interactions [13, 20].

The nucleus-electron coupling of interest in solid TISCN is divided into two parts: The chemical shift interaction and the nucleus-electron indirect interaction. For the former interaction we are concerned only with its anisotropic part, and the relaxation rate  $R^{\text{CSA}} \{=(T_1^{\text{CSA}})^{-1}\}$  due to this interaction is given by [20, 21]

$$R^{\text{CSA}} = (2/15) \omega^2 (\delta_{\parallel} - \delta_{\perp})^2 j(\omega), \quad (1)$$

$$j(\omega) = \tau / (1 + \omega^2 \tau^2). \quad (2)$$

Here, the chemical shift tensor is assumed to be axially symmetric and  $\delta_{\parallel}$  and  $\delta_{\perp}$  refer to the shielding along and perpendicular to the symmetry axis, respectively.  $\omega$  stands for the Larmor frequency of  $^{203}\text{Tl}$  or  $^{205}\text{Tl}$  nuclei and  $\tau$  is the correlation time of the time-dependent fluctuation of interest.

The nucleus-electron indirect interaction can be subdivided into scalar (or exchange) and pseudodipolar terms. The scalar coupling between unlike spins contributes to the second moments as well as to the relaxation but the one between like spins does not [17–20, 22]. The relaxation rate of spin  $i$  ( $R_i^{\text{SC}}$ ) due to

the scalar interaction is [20]

$$R_i^{\text{SC}} = (2/3) \sum_j A_{ij}^2 S_j (S_j + 1) j(\omega_i - \omega_j), \quad (3)$$

where  $A_{ij}$  is the scalar coupling constant, in units of rad/s, between  $i$  and unlike  $j$  spins, of which the Larmor frequencies are expressed by  $\omega_i$  and  $\omega_j$ , respectively, and  $S_j$  is the spin quantum number of spin  $j$ . The sum of  $A_{ij}^2$  can be expressed by the second moment of  $i$  spins due to the same interaction by [17–19]

$$\langle \delta \omega^2 \rangle_i^{\text{SC}} = (1/3) \sum_j A_{ij}^2 S_j (S_j + 1). \quad (4)$$

From the natural abundances of the Tl isotopes,  $\langle \delta \omega^2 \rangle_{203}^{\text{SC}}$  is expected to be 2.4 times larger than  $\langle \delta \omega^2 \rangle_{205}^{\text{SC}}$ . The observed ratio of  $T_2^*$  shows that the dominant interaction in solid TISCN is the scalar one.

The pseudodipolar term can be approximated by the same expression as that for the normal dipolar interaction except for its coupling constant, and these two interactions are combined into a single term [18, 19]. For several Tl-containing compounds, the scalar interaction is estimated to be larger than the pseudodipolar interaction as well as than the normal dipolar interaction between Tl nuclei [17–19]. In the following discussion we neglect the pseudodipolar interaction as well.

Because the two spin systems of  $^{203}\text{Tl}$  and  $^{205}\text{Tl}$  couple to each other, the observed relaxation rates are the eigen values of the following relaxation matrix [17, 20]:

$$\begin{pmatrix} -R^{\text{CSA}} - R_{203}^{\text{SC}} & R_{203}^{\text{SC}} \\ R_{205}^{\text{SC}} & -R^{\text{CSA}} - R_{205}^{\text{SC}} \end{pmatrix}. \quad (5)$$

Here,  $R^{\text{CSA}}$  is assumed to be the same for  $^{203}\text{Tl}$  and  $^{205}\text{Tl}$ , and a small difference (less than 1%) in their gyromagnetic ratios is neglected for simplicity. As a result, one can obtain two characteristic  $T_1$  values:

$$(T_1^s)^{-1} = R^{\text{CSA}} + R^{\text{SC}}, \quad (6)$$

$$(T_1^l)^{-1} = R^{\text{CSA}}, \quad (7)$$

where

$$R^{\text{SC}} = R_{203}^{\text{SC}} + R_{205}^{\text{SC}} = 2 (C^{\text{SC}})^2 j(\omega_{203} - \omega_{205}), \quad (8)$$

$$C^{\text{SC}} = (\langle \delta \omega^2 \rangle_{203}^{\text{SC}} + \langle \delta \omega^2 \rangle_{205}^{\text{SC}})^{1/2}. \quad (9)$$

Therefore, the observed relaxation times,  $T_1^s$  and  $T_1^l$ , become isotope independent. This is the case, as described in the previous section.

As discussed later,  $T_1^1$  below 350 K is likely to change as

$$(T_1^1)^{-1} = K T^2. \quad (10)$$

This type of  $T_1$  behavior may be assigned to the relaxation by lattice vibrations via a Raman-like process [13, 17, 20]. Therefore, the contribution of (10) is added to (7).

Now, we will consider the correlation time  $\tau$  of the head-to-tail flip of the linear  $\text{SCN}^-$  ions in the TISCN crystal, which is the most interesting motion in the phase transition. Phase I of TISCN is tetragonal with the space group  $I4/mcm$  [10]. The site symmetries require that the  $\text{SCN}^-$  ion in phase I is disordered between two equivalent orientations, implying that the anionic head-to-tail flip is occurring between symmetric potential wells. Even in phase II, the flip is assumed to go on, but it occurs between unequal potential wells.

Simplified potential curves are shown in Figure 4. Between the asymmetric potential wells for phase II, the  $\text{SCN}^-$  ion jumps with a rate  $W$  from a favored to unfavored orientation and with a rate  $aW$  in the opposite direction.

$$W = k \exp \{ -(E_a + \Delta E)/RT \}, \quad (11)$$

$$a = \exp (2 \Delta E/RT). \quad (12)$$

The usual Arrhenius relation is used for the jump rates. The parameter  $a$  represents the ratio of the statistical probabilities that the  $\text{SCN}^-$  ion occupies the favored and the unfavored orientation and is related to the order parameter  $\eta$  by

$$\eta = (a - 1)/(a + 1). \quad (13)$$

The correlation time of the motion is defined as

$$\tau^{-1} = W + aW, \quad (14)$$

$$\tau = \tau_0 \exp \{ (E_a + \Delta E)/RT \} / (1 + a). \quad (15)$$

Finally, the observed  $T_1^{-1}$  given by (6) and (7) should be corrected by a factor of  $4a/(1+a)^2$  because of the smaller occupancy of the unfavored orientation [23]. For the symmetric potential, of course,  $\Delta E = 0$ ,  $a = 1$ , and  $\eta = 0$ .

#### $T_1^1$ in Phases I and II

The temperature dependence of  $T_1^1$  can be separated into two regions: The low-temperature region where  $T_1^1$  shows no frequency dependence and the high-tem-

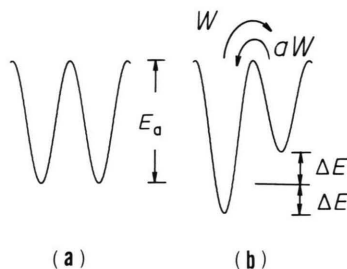


Fig. 4. Scheme of the potential curves for the head-to-tail flip of an  $\text{SCN}^-$  ion (a) in the disordered high-temperature phase I and (b) in the ordered low-temperature phase II.

perature region where  $T_1^1$  has a frequency dependent minimum. At temperatures below 350 K,  $T_1^1$  changed according to (10), where  $K = 3.4 \cdot 10^{-6} \text{ s}^{-1} \text{ K}^{-2}$ , and is attributed to the lattice vibrations. The relaxational behavior given by (10) is frequently observed in  $T_1$  for nuclei with  $I \geq 1$  having a nuclear electric quadrupole moment [24]. Because both Tl nuclei have no quadrupole moment, the interactions modulated by the lattice vibrations are of magnetic origin, maybe due to indirect nucleus-electron interactions between the Tl nuclei, which depend on Tl-Tl distances more strongly than the normal dipolar ones [18].

The  $T_1^1$  minima in phase I are characteristic for relaxation due to the chemical shift anisotropy given by (1). The temperature and frequency dependence of  $T_1^1$  were analyzed in this line, and the motional parameters responsible for the  $T_1^1$  minima were determined by a least-squares fitting of (1) and (10). The numerical results are listed in Table 1, and the calculated  $T_1^1$  dependence is given in Figure 2. It is reasonable to assign the observed  $E_a$  and  $\tau_0$  to the head-to-tail flips of the  $\text{SCN}^-$  ions because translational self-diffusion of the  $\text{Tl}^+$  ions was detected through  $T_1^s$  as discussed later.

It is still not clear whether the cation in phase I exists in ordered positions or not [3, 7, 10]. Two models are proposed: One implies that  $\text{Tl}^+$  is fixed at 0, 0, 1/4 sites on the crystal  $C_4$  axis, and the other assumes that the cation occupies four sites statistically and dynamically with equal occupancy 1/4. The four sites are slightly displaced from the 0, 0, 1/4 site and related to each other by the  $C_4$  symmetry. Here, we observed a rather large effect from the chemical shift anisotropy on Tl  $T_1$ . This fact excludes the former model for the  $\text{Tl}^+$  positions, because the chemical shift tensor for the  $\text{Tl}^+$  ion fixed on the  $C_4$  axis is invariant under the simple  $180^\circ$  flip of the anions. Therefore, the



| Phase | $T_1$   | $ \delta_{  } - \delta_{\perp} $<br>ppm | $C^{\text{SC}}$<br>krad/s | $E_a$<br>kJ mol <sup>-1</sup> | $2\Delta E$<br>kJ mol <sup>-1</sup> | $\tau_0$<br>10 <sup>-14</sup> s | $K$<br>10 <sup>-6</sup> s <sup>-1</sup> K <sup>-2</sup> |
|-------|---------|---|---------------------------|-------------------------------|-------------------------------------|---------------------------------|---|
| I     | $T_1^1$ | 341                                     | —                         | 50.5                          | 0                                   | 1.70                            | 4.0   |
|       | $T_1^s$ | —                                       | 9.0                       | 54.4                          | 0                                   | 1.98                            | —   |
| II    | $T_1^1$ | —                                       | —                         | —                             | —                                   | —                               | 3.4   |
|       | $T_1^s$ | —                                       | 9.0 <sup>a</sup>          | 54.4 <sup>a</sup>             | 5.5 <sup>b</sup>                    | 1.98 <sup>a</sup>               | —   |

Table 1. Motional parameters in solid TlSCN.

<sup>a</sup> These are taken to be equal to the corresponding ones determined from  $T_1^s$  in phase I.

<sup>b</sup> This is fixed below 325 K.

$\text{TI}^+$  ion in phase I should be disordered dynamically over the four positions. This conclusion supports the model of positional disorder of  $\text{TI}^+$  or the “dynamical twinning model” [10]. Then the direct origin of the modulation of the chemical shift anisotropy at the TI sites may be attributed to a local hopping of the  $\text{TI}^+$  ions, which is closely correlated to the head-to-tail flips of the  $\text{SCN}^-$  ions.

#### $T_1^s$ in Phase I

The temperature dependence of  $T_1^s$  between  $T_c$  and 435 K in phase I can be analyzed in terms of the same model as above, but the interaction considered is scalar. The theoretical  $T_1^s$  is given by (6), indicating no isotope but frequency dependence. By fitting (6) to the data in this temperature region, three motional parameters  $C^{\text{SC}}$ ,  $\tau_0$ , and  $E_a$  were determined.  $\tau_0$  and  $E_a$  determined from  $T_1^s$  are in reasonable agreement with those from  $T_1^1$ . Thus, we could determine the motional parameters of the anionic flips indirectly through the TI NMR relaxations. An  $E_a$  value of the  $\text{SCN}^-$  ion flip has been determined for KSCN by means of the temperature dependence of the Raman linewidth [5] and  $^{39}\text{K}$   $T_1$  [8] as ca. 40 kJ mol<sup>-1</sup>. The value of 51–54 kJ mol<sup>-1</sup> for TlSCN is somewhat large in comparison with that for KSCN. This may reflect the smaller  $c$  axis of phase I of TlSCN compared to KSCN [7, 10], taking into account that out-of-plane flips of the  $\text{SCN}^-$  ions are dominant rather than in-plane ones [1, 7].

Above 435 K in phase I,  $T_1^s$  at 16 MHz decreased sharply with increasing temperature. This  $T_1^s$  decrease is assignable to the translational self-diffusion of  $\text{TI}^+$  ions, because a substantial motional narrowing was observed in the temperature dependence of  $T_2^*$  in the same temperature range (Figure 3). To confirm this, we preliminarily measured the electrical conductivity by an ac impedance method and found it to be as high as  $2 \cdot 10^{-4} \text{ S m}^{-1}$  at ca. 460 K, supporting the occurrence of rapid ionic diffusion. The  $E_a$  value of the  $\text{TI}^+$

ionic diffusion was roughly estimated from  $T_1^s$  to be 90 kJ mol<sup>-1</sup>. This  $E_a$  value in TlSCN is comparable with 77 kJ mol<sup>-1</sup> for the high-temperature phase of  $\text{TlNO}_3$  [17] but much smaller than 48 kJ mol<sup>-1</sup> in the high-temperature phase of  $\text{TlNO}_2$  [13]. The small value for the latter compound is attributable to the fact that its conducting phase is an ionic plastic phase [25].

#### $T_1^s$ in Phase II and the Order Parameter

Since  $T_1^s$  changes smoothly through  $T_c$  and shows a flat minimum below  $T_c$ , it is obvious that the  $\text{SCN}^-$  ion is still rapidly flipping even in the low-temperature ordered phase I. The interaction responsible to the  $T_1^s$  relaxation is also the scalar one, but the potential curve for flips becomes asymmetric as shown in Figure 4b. The analysis of the  $T_1^s$  data can be made by using (6) and (13–15) to determine the unknown parameters  $E_a$ ,  $\tau_0$ ,  $C^{\text{SC}}$ , and  $\Delta E$ .

First, we tried to fit the theoretical  $T_1^s$  to the observed ones, adjusting the above four constants. The calculations gave a good fitness between the experimental and observed curves but yielded a unreasonably large  $C^{\text{SC}}$  value (ca. 480 k rad/s), compared with 9.0 k rad/s for phase I and also with the values reported for  $\text{TlNO}_2$  [13],  $\text{TlCl}$  [19], or  $\text{TlNO}_3$  [17]. Therefore, this model calculation was disregarded. Secondly, we adopted a model for which  $\Delta E$  is temperature dependent. This model is closely related to the order-disorder transition mechanism. For the simplicity of the analysis and also to retain the continuity of the  $T_1^s$  through  $T_c$ , we assumed that the values of  $C^{\text{SC}}$ ,  $E_a$ , and  $\tau_0$  are the same as the corresponding ones determined from  $T_1^s$  in phase I. Then, we calculated the theoretical  $T_1^s$  to fit the low-temperature portion of the observed  $T_1^s$  by varying  $\Delta E$ . This procedure implies that  $\Delta E$  is temperature independent at temperatures much below  $T_c$ . The  $T_1^s$  curves thus obtained are drawn in Figure 2. The temperature dependent  $\Delta E$  or  $\eta$  can be estimated from the difference between the

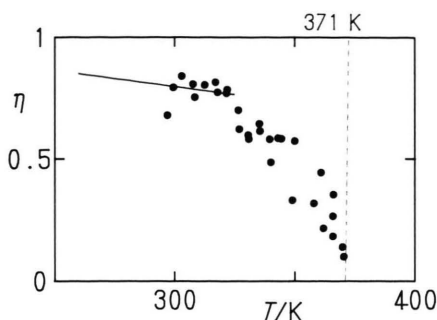


Fig. 5. Temperature dependence of the order parameter  $\eta$  determined from  $T_1^s$  for phase II of TISCN. The curve below 325 K is calculated from (12) and (13) with a temperature independent  $2\Delta E$  of  $5.5 \text{ kJ mol}^{-1}$ .

observed and calculated  $T_1^s$ , and the result is shown in Figure 5. The  $\eta$  vs.  $T$  curve indicates a first-order phase transition.

In conclusion, the temperature dependence of the Tl spin-lattice relaxation times in solid TISCN can be analyzed in terms of the chemical shift anisotropy at the Tl nuclei and the scalar interaction between the  $^{203}\text{Tl}$  and  $^{205}\text{Tl}$  nuclei modulated by the head-to-tail flips of the linear  $\text{SCN}^-$  ions. The motional parameters of the anionic flip were determined indirectly from the Tl  $T_1^s$  and  $T_1^l$  for the high-temperature phase I. For the low-temperature phase II, the order parameter of the  $\text{SCN}^-$  ion orientation could be determined, confirming the order-disorder nature of the phase transition. It should be emphasized, however, that the order parameters are derived under several assumptions and have large scatter because of the difficulty in determining  $T_1^s$  precisely from the nonexponential  $T_1$  recovery.

- [1] M. Sakiyama, H. Suga, and S. Seki, *Bull. Chem. Soc. Japan* **36**, 1025 (1963).
- [2] Y. Kinsho, N. Onodera, M. Sakiyama, and S. Seki, *Bull. Chem. Soc. Japan* **52**, 395 (1979).
- [3] Y. Yamada and T. Watanabe, *Bull. Chem. Soc. Japan* **36**, 1032 (1963).
- [4] Z. Iqbal, L. H. Sarma, and K. D. Möller, *J. Chem. Phys.* **57**, 4728 (1972).
- [5] F. J. Owens, *Solid State Commun.* **29**, 789 (1979).
- [6] S. Yamamoto, M. Sakuno, and Y. Shinnaka, *J. Phys. Soc. Japan* **56**, 2604 (1987).
- [7] S. Yamamoto, M. Sakuno, and Y. Shinnaka, *J. Phys. Soc. Japan* **56**, 4393 (1987).
- [8] B. Topič, U. Haeberlen, R. Blinc, A. Fuith, and H. Warhanek, *Solid State Commun.* **72**, 151 (1989).
- [9] W. Klement, Jr., *Bull. Chem. Soc. Japan* **49**, 2148 (1976).
- [10] R. Lippman and R. Rudman, *J. Chem. Phys.* **79**, 3457 (1983).
- [11] S. Manolatos, M. Tillinger, and B. Post, *J. Solid State Chem.* **7**, 31 (1973).
- [12] T. Tanabe, R. Ikeda, and D. Nakamura, *Phys. Stat. Sol.* **a114**, K143 (1989).
- [13] Y. Furukawa and H. Kiriya, *Chem. Phys. Lett.* **93**, 617 (1982).
- [14] S. Gima, Y. Furukawa, R. Ikeda, and D. Nakamura, *J. Mol. Struct.* **111**, 189 (1983).
- [15] Y. Kume, R. Ikeda, and D. Nakamura, *J. Magn. Resonance* **33**, 331 (1979).
- [16] M. M. Markowitz, *J. Org. Chem.* **22**, 983 (1957).
- [17] M. Villa and A. Avogadro, *Phys. Stat. Sol.* **b75**, 179 (1976).
- [18] N. Bloembergen and T. J. Rowland, *Phys. Rev.* **97**, 1679 (1955).
- [19] S. Clough and W. I. Goldberg, *J. Chem. Phys.* **45**, 4080 (1966).
- [20] A. Abragam, *The Principles of Nuclear Magnetism*, Oxford Univ. Press, Oxford 1961, Chapter 8.
- [21] T. C. Farrar and E. D. Becker, *Pulse and Fourier Transform NMR*, Academic Press, New York 1971, Chapter 4.
- [22] J. H. Van Vleck, *Phys. Rev.* **74**, 1168 (1948).
- [23] D. C. Look and I. J. Lowe, *J. Chem. Phys.* **44**, 3437 (1966).
- [24] H. Chihara and N. Nakamura, *Adv. Nucl. Quadrupole Resonance* **4**, 1 (1980).
- [25] K. Moriya, T. Matsuo, and H. Suga, *J. Phys. Chem. Solids* **44**, 1103 (1983).